

Amorphous vs crystalline exciton blocking layers at the anode interface in planar and planar-mixed heterojunction organic solar cells

Stefan Grob, Mark Gruber, Andrew N. Bartynski, Ulrich Hörmann, Theresa Linderl, Mark E. Thompson, Wolfgang Brütting

Angaben zur Veröffentlichung / Publication details:

Grob, Stefan, Mark Gruber, Andrew N. Bartynski, Ulrich Hörmann, Theresa Linderl, Mark E. Thompson, and Wolfgang Brütting. 2014. "Amorphous vs crystalline exciton blocking layers at the anode interface in planar and planar-mixed heterojunction organic solar cells." Applied Physics Letters 104 (21): 213304. <https://doi.org/10.1063/1.4879839>.

Nutzungsbedingungen / Terms of use:

licgercopyright

Dieses Dokument wird unter folgenden Bedingungen zur Verfügung gestellt: / This document is made available under the following conditions:

Deutsches Urheberrecht

Weitere Informationen finden Sie unter: / For more information see:

<https://www.uni-augsburg.de/de/organisation/bibliothek/publizieren-zitieren-archivieren/publizieren>



Amorphous vs crystalline exciton blocking layers at the anode interface in planar and planar-mixed heterojunction organic solar cells

Cite as: Appl. Phys. Lett. **104**, 213304 (2014); <https://doi.org/10.1063/1.4879839>

Submitted: 22 April 2014 . Accepted: 14 May 2014 . Published Online: 28 May 2014

Stefan Grob, Mark Gruber, Andrew N. Bartynski, Ulrich Hörmann, Theresa Linderl, Mark E. Thompson, and Wolfgang Brütting



View Online



Export Citation



CrossMark

ARTICLES YOU MAY BE INTERESTED IN

[Small molecular organic photovoltaic cells with exciton blocking layer at anode interface for improved device performance](#)

Applied Physics Letters **99**, 153302 (2011); <https://doi.org/10.1063/1.3650472>

[Two-layer organic photovoltaic cell](#)

Applied Physics Letters **48**, 183 (1986); <https://doi.org/10.1063/1.96937>

[A hybrid planar-mixed tetraphenyldibenzoperiflanthene/C₇₀ photovoltaic cell](#)

Applied Physics Letters **102**, 073302 (2013); <https://doi.org/10.1063/1.4793195>

Lock-in Amplifiers

... and more, from DC to 600 MHz



Amorphous vs crystalline exciton blocking layers at the anode interface in planar and planar-mixed heterojunction organic solar cells

Stefan Grob,^{1,a)} Mark Gruber,¹ Andrew N. Bartynski,² Ulrich Hörmann,¹ Theresa Linderl,¹ Mark E. Thompson,² and Wolfgang Brütting^{1,b)}

¹Institute of Physics, University of Augsburg, 86135 Augsburg, Germany

²Department of Chemical Engineering and Department of Chemistry, University of Southern California, Los Angeles, California 90089, USA

(Received 22 April 2014; accepted 14 May 2014; published online 28 May 2014)

We compare the gain in power conversion efficiency (PCE) achieved by inserting either amorphous or crystalline exciton blocking layers at the anode interface for planar (PHJ) and planar-mixed heterojunction (PM-HJ) organic solar cells based on Tetraphenyldibenzoperiflanthene and fullerenes. For PHJ devices, there is a gain of more than 37% for both types of blocking layers, mainly due to an increase in photocurrent, indicating that this gain can be solely ascribed to the exciton blocking effect. A templating effect as proposed in literature for crystalline blocking layers cannot be affirmed. On the contrary, it is shown that there is a connection between the choice of acceptor (C_{60}/C_{70}) and the blocking effect on the anode side. Moreover, we can show that also for PM-HJ devices a remarkable efficiency enhancement is possible. The insertion of suitable blocking layers at the anode interface can alter the effective work function and thus the open-circuit voltage, leading to a maximum PCE of 5.8% in single junction cells. © 2014 AIP Publishing LLC. [<http://dx.doi.org/10.1063/1.4879839>]

The use of exciton blocking layers in organic donor-acceptor solar cells is well established, however, so far the focus has mainly been on the cathode. There, such blocking layers are mandatory as they prevent the penetration of subsequently evaporated cathode material (e.g., Al, Ag) into the active layer. In addition, the application of materials like bathocuproine (BCP^{1,2}) or bathophenanthroline (BPhen^{3,4}) also enhances the efficiency of organic solar cells by suppressing exciton-quenching at the metal-organic interface. At the opposite contact, it is also common to insert a buffer layer consisting of, e.g., MoO_x or poly(ethylenedioxythiophene):poly(styrenesulfonate) (PEDOT:PSS) between anode - which is usually built up on indium tin oxide (ITO) - and donor material. This is done because ITO alone, due to its insufficient work function, cannot act as the desired hole-selective contact leading to high leakage currents. But it is usually neglected that, like ITO itself, these buffer layers are also exciton quenchers due to their quasi-metallic nature.

For planar heterojunction (PHJ) organic solar cells, it has already been shown that this recombination channel can be suppressed by inserting either crystalline⁵ or amorphous blocking layers,⁶ resulting in higher power conversion efficiencies (PCE) by notably elevating the short-circuit current density (J_{SC}), while leaving the values of open-circuit voltage (V_{OC}) and fill factor (FF) almost unchanged. It was also suggested that the use of crystalline blockers as a nanostructured template could increase the area of the donor/acceptor interface, which would further enhance J_{SC} , indicating that crystalline blockers are more favorable.⁵

In this work, we seek to clarify the influence of morphology by comparing blocking layers consisting of either crystalline diindenoperylene (DIP) or amorphous N,N' -bis(naphthalen-1-yl)- N,N' -bis(phenyl)-2,2'-dimethylbenzidine

(α -NPD) in planar as well as in planar-mixed heterojunction (PM-HJ) devices. The blocking materials are selected based on the alignment of their energy levels related to highest occupied molecular orbital (HOMO) and lowest unoccupied molecular orbital (LUMO) of the donor material. To achieve hole transport and efficient exciton blocking simultaneously, the ionization potential must be smaller (or at least similar), while its energy gap has to be wider compared to the donor. To emphasize the blocking effect, a highly absorbing donor material is chosen. Tetraphenyldibenzoperiflanthene (DBP⁷) has already been proven to form efficient solar cells in combination with fullerenes providing high PCEs up to 8.1%.⁸ Its ability to absorb efficiently is due to the horizontal orientation of the molecules, which enables a strong coupling between the incident light and the transition dipole moment, which is aligned along the long axis of the molecule.⁹ As electron acceptor material, we mainly used the fullerene C_{60} . However, some selected cells were fabricated using the stronger absorbing fullerene C_{70} to achieve a maximum PCE of $5.8\% \pm 0.2\%$ in single junction cells.

Fig. 1 shows the used organic materials with their energy levels and absorption spectra. The PEDOT:PSS derivative HIL1.3 was obtained from Clevios (Germany), α -NPD and DBP from Lumtec (Taiwan), DIP from S. Hirschmann (Univ. Stuttgart, Germany), and BCP from Sigma-Aldrich. HIL1.3 was spin-coated from aqueous dispersion and subsequently dried at 125 °C for 30 min. All other materials were evaporated in UHV ($< 5 \times 10^{-7}$ millibars) at 0.5 Å/s. Current-voltage (J-V) characteristics were recorded using a source measure unit (Keithley 236 SMU) under illumination with a solar simulator (Oriel 300 W with AM 1.5 G filters) in a glovebox system with nitrogen atmosphere. The illumination intensity was approved by a calibrated silicon reference cell (RERA systems, PV Measurement Facility, Radboud University Nijmegen, area $1 \times 1 \text{ cm}^2$). Incident photon-to-current efficiency (IPCE)

^{a)}Electronic mail: stefan.grob@physik.uni-augsburg.de

^{b)}Electronic mail: wolfgang.brueetting@physik.uni-augsburg.de

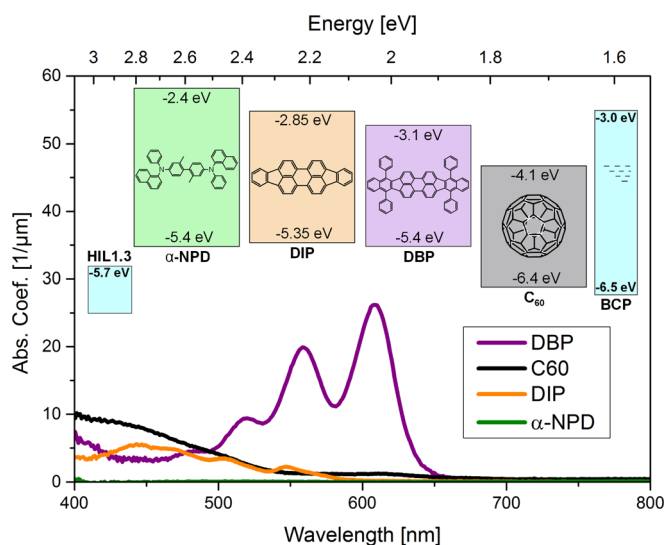


FIG. 1. Schematic drawing of molecular formulae and energy levels of α -NPD, DIP, DBP, and C_{60} . Energy values of organic materials are taken from literature.^{10,11} Moreover the absorption characteristics of donor, acceptor, and blocking materials are shown, with DBP featuring the by far most dominant absorption, while DIP and α -NPD absorb only weakly.

measurements were carried out using a monochromatized Xe arc lamp as light source and lock-in detection.

Generally, the architecture of the PHJ solar cells is ITO (140 nm)/HIL1.3 (45 nm)/blocking layer (y nm)/DBP (15 nm)/fullerene (45 nm)/BCP (5 nm)/Al (100 nm), i.e., the only variables are the blocking layer material and the thickness of that layer. DIP is chosen to form the crystalline blocking layer, exhibiting exceptionally high structural order in evaporated thin films.¹² The DIP molecule, consisting of seven benzene and two cyclopentadiene rings, also forms the backbone of the DBP molecule, resulting in similar optical spectra. Nevertheless, there are significant differences. The DBP molecule has one further benzene ring on each side, increasing the π -electron system and thus leading to a red-shift of absorption and therefore a smaller energy gap. Moreover, it features four additional, rotatable phenyl groups, changing the molecular orientation within the layer and by that the absorption coefficient (Fig. 1). Nevertheless, both requirements for effective exciton blocking are met: The energy gap for DIP is wider, as absorption measurements reveal, while UPS measurements show identical HOMO-offsets for DIP/ C_{60} and DBP/ C_{60} as required for hole transport to the anode. Due to its high order in evaporated thin films with large exciton diffusion lengths of up to 100 nm,¹³ DIP is also used as donor material in organic solar cells, yielding exceptionally high fill factors of nearly 75%.¹⁴ However, the almost upright standing alignment of the DIP molecules leads to weak absorption and therefore a much smaller J_{SC} compared to DBP. This weak absorption is also advantageous in blocking layers, otherwise parasitic absorption can occur and the gain in current could not solely be ascribed to decreasing quenching effects. We excluded the impact of DIP absorption by varying the thickness of the blocking layer from 3 to 21 nm in 3 nm steps receiving almost identical values for J_{SC} (Fig. 2(a)). This result leads to the assumption that 3 nm of DIP already forms a (nearly) closed layer, which is in accordance with investigations,

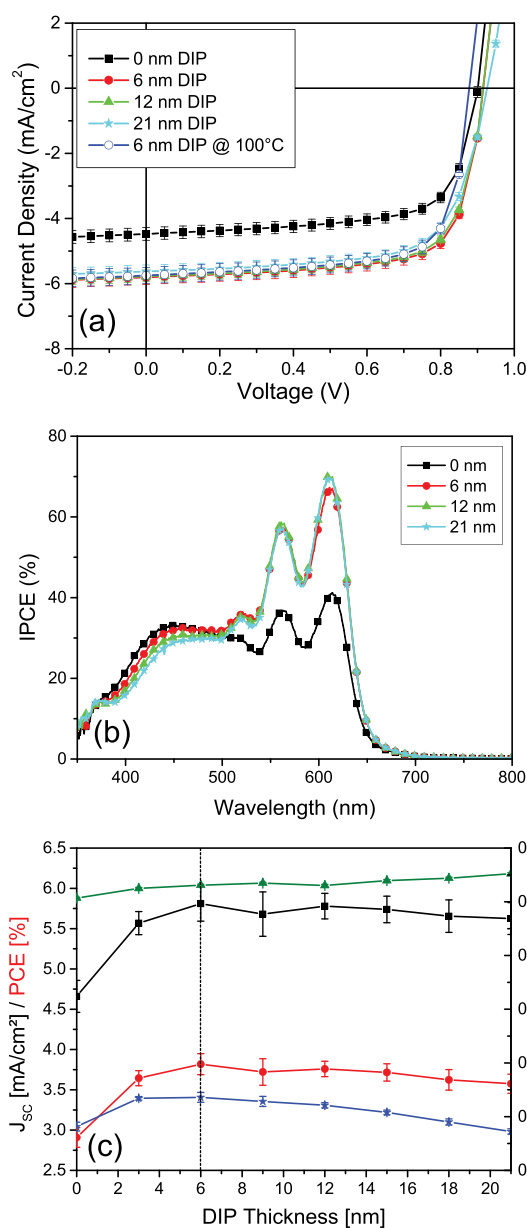


FIG. 2. (a) J - V -characteristics, (b) IPCE curves and (c) solar cell parameters vs thickness of the DIP blocking layer. The architecture of the PHJ solar cells is ITO(140 nm)/HIL1.3(45 nm)/DIP(x nm)/DBP(15 nm)/ C_{60} (45 nm)/BCP(5 nm)/Al(100 nm). For reasons of clarity, some curves were omitted in (a) and (b).

revealing the tendency of DIP to grow in Stranski-Krastanov mode on various substrates.^{15,16} Compared to the reference without blocking layer, the gain in J_{SC} is between a minimum of 24% (3 nm DIP) and a maximum of 30% (6 nm DIP), staying nearly constant for higher thicknesses of the DIP layer. Moreover, also the values for V_{OC} (continuously) and FF (at first) show a small increase (Fig. 2(c)). This slight but continuous gain in V_{OC} for thicker blocking layers is an additional effect of the reduced recombination,¹⁷ whereas the fill factor increases from 69% (0 nm) to a maximum of 72% (6 nm) but then decreases again down to its initial value (21 nm) due to transport issues.

The PCE increases from 2.8% for the reference up to 3.8% for the best cell in this series containing a 6 nm DIP blocking layer, an improvement of more than 37%. Furthermore, the similarity of the J - V -characteristics of the

compared solar cells leads to the conclusion that a possible template effect is not relevant. Due to pronounced island growth for higher DIP thicknesses, the root mean square roughness for the DIP/DBP interface increases, however, this effect does not propagate to the DBP/fullerene interface, where it could lead to enhanced exciton dissociation and thus a higher J_{SC} . As well, AFM images and XRD measurements (not shown) do not reveal any signs of changed morphology and structure of the DBP layer. Even for DIP grown at elevated temperatures ($T_{Substrate} = 100^\circ\text{C}$), which leads to an enhanced lateral crystallinity of the DIP layer,¹⁸ no changes in J_{SC} can be observed (open symbols in Fig. 2(a)). Therefore, the by far most dominant effect for the gain in J_{SC} is reduced exciton quenching at the HIL1.3/organic interface, which is also supported by IPCE measurements (Fig. 2(b)), revealing that the increment is mainly at wavelengths (λ) between 500 nm and 650 nm, where the maximum absorption of DBP occurs (Fig. 1). In the main absorption region of C_{60} ($400\text{ nm} < \lambda < 500\text{ nm}$), however, only small differences between the IPCE curves are visible. This is in accordance with the assumption that less excitons generated within the DBP layer are quenched at the HIL1.3 buffer layer, but instead dissociate at the DBP/ C_{60} interface, generating free charge carriers.

N,N' -bis(naphthalen-1-yl)- N,N' -bis(phenyl)-2,2'-dime-thylbenzidine (α -NPD) also fulfills the requirements for efficient blocking layers in combination with DBP concerning energy level alignment and hole transporting ability, while hardly absorbing itself in the visible range. In contrast to highly crystalline DIP, thermally evaporated α -NPD forms amorphous thin films.¹⁹ As there is no template effect for DIP, a similar gain in J_{SC} for amorphous blockers is expected. This assumption can be verified by the J - V -characteristics (Fig. 3(a)). For the best cell with a 9 nm thick α -NPD layer, J_{SC} increases by 29%. Compared to the 30% of the device exhibiting 6 nm DIP, one can state that there is no difference in J_{SC} between devices with crystalline or amorphous blocking layers within the range of error. Moreover, the same trends for V_{OC} and FF can be observed compared to devices with crystalline blocking layer (Fig. 3(c)), so that there is again an increase in PCE of about 37%. This leads to the conclusion that a possible template effect of crystalline blocking layers as proposed in literature⁵ is not occurring or at least its impact is negligible. However, there is a big difference in the thickness dependence of device parameters between these two blocking layers. While there was hardly any correlation between layer thickness and device performance for the DIP-containing solar cells, this is not the case for the α -NPD devices. This is connected with two factors. First, it is assumed that 3 and even 6 nm of α -NPD are not sufficient to form a closed layer, which leads to incomplete blocking and thus less gain in J_{SC} compared to structurally identical DIP devices. Second, blocking layers exceeding 9 nm show an increasing s-shape behavior.

We ascribe this feature to a growing transport resistance,²⁰ an effect which is naturally much more pronounced for amorphous films as they generally feature lower charge carrier mobilities. To confirm, samples with 21 nm α -NPD highly doped with MoO_x (9:1 and 4:1) were prepared. As a result, the s-shape vanishes (open symbols in Fig. 3(a)). However, as MoO_x also acts as a quencher, J_{SC} decreases

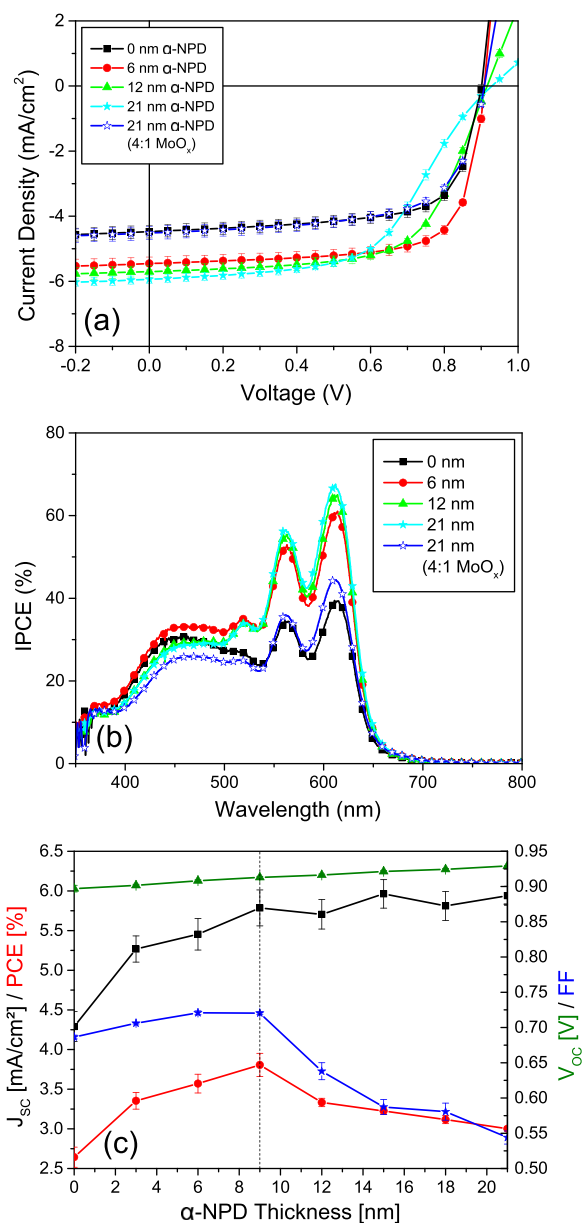


FIG. 3. (a) J - V -characteristics, (b) IPCE curves and (c) solar cell parameters vs thickness of the α -NPD blocking layer. The architecture of the PHJ solar cells is ITO(140 nm)/HIL1.3(45 nm)/ α -NPD(x nm)/DBP(15 nm)/ C_{60} (45 nm)/BCP(5 nm)/Al(100 nm). Again, for reasons of clarity, some curves were omitted in (a) and (b).

again with increasing percentage of MoO_x . The quenching effect is also revealed by the corresponding IPCE characteristics (open symbols in Fig. 3(b)). IPCE curves naturally show the same trend as J_{SC} with an increasing amount of generated charge carriers up to a layer thickness of 9 nm and a following saturation for thicker blocking layers.

Mixing donor and acceptor molecules to enhance their interface resulting in more efficient exciton dissociation is a well-established concept.^{21,22} In this work, so-called planar-mixed heterojunction devices were prepared, a combination of strictly planar and bulk heterojunction devices, combining the benefits of both concepts.²³ This means that a mixed layer of DBP and C_{60} is sandwiched between a DBP layer on the anode and a C_{60} layer on the cathode side. Furthermore, devices with added blocker layer and skipping the pure DBP layer were fabricated. The volume ratio DBP:fullerene in the

bulk was chosen 1:2, as this composition has proven to provide high PCEs for this material combination.²⁴

In contrast to PHJ devices, there are significant differences in J - V -characteristics comparing crystalline DIP and amorphous α -NPD as blocking layers (Figure 4(a)). As the main difference concerns V_{OC} , this is not related to the morphology of the blockers but can be associated to shifting energy levels and a change of the effective work function of the anode. Compared to PHJ devices, already the V_{OC} of the reference PM-HJ cell without blocker drops from 0.90 V to 0.84 V, which declines further to 0.79 V introducing a DIP layer and even to 0.76 V by additionally skipping the pure DBP layer. The opposite effect is observed inserting α -NPD. In these cells, V_{OC} increases to the value of the PHJ cell, lying a little bit higher for the cell without the neat DBP layer.

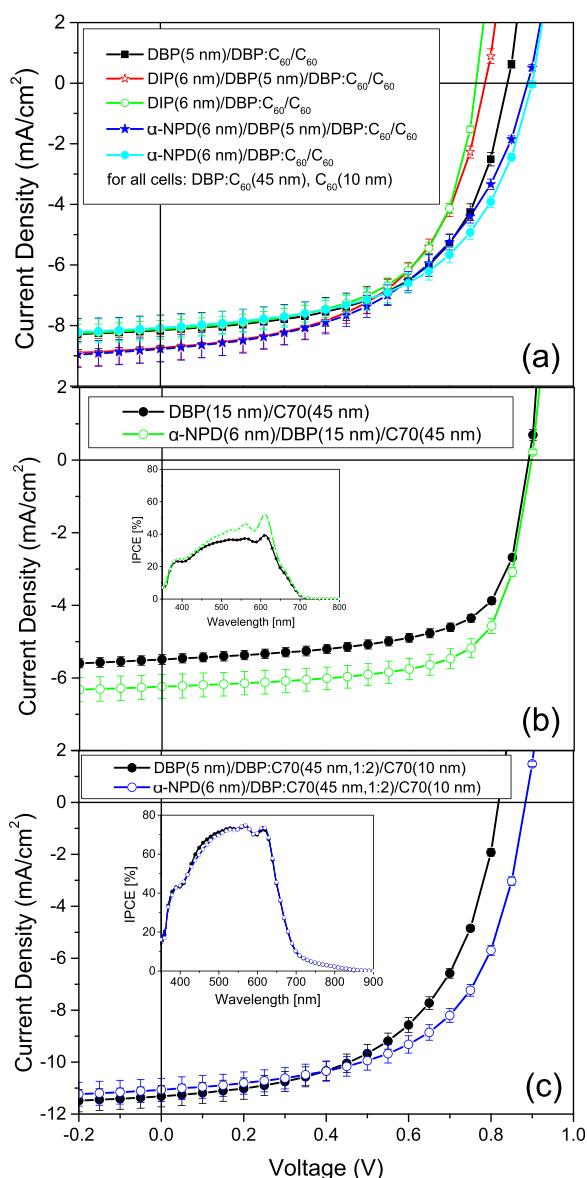


FIG. 4. J - V -characteristics of (a) DBP/C₆₀ PM-HJ devices (volume ratio 1:2), (b) DBP/C₇₀ PHJ devices, and (c) DBP/C₇₀ PM-HJ solar cells. The insets in (b) and (c) show the related IPCE curves. The architecture of the solar cells is ITO(140 nm)/HIL1.3(45 nm)/organic/BCP(5 nm)/Al(100 nm), with the active organic layers explained within each diagram.

For J_{SC} again there is an increase upon introduction of the blocker layer, however, it is smaller compared to that in PHJ devices. This is explained by the more efficient exciton dissociation already given by the device architecture, leading to less excitons reaching the blocking layer interface. Despite that gain in J_{SC} there is hardly any rise in PCE as the cells showing a higher current either lack in V_{OC} (DIP, open stars) or in FF (α -NPD, filled stars). The cells without the pure DBP layers show the same J_{SC} as the reference. This is due to the fact that blocking excitons with DIP or α -NPD compensates additional absorption of the thin DBP layer. Thus, the best cell in this series is the α -NPD/DBP:C₆₀/C₆₀ device, showing a small increase in PCE from 3.9% of the cell without blocking layer to 4.0%, mainly due to the gain in V_{OC} .

Naturally, there is a close connection between the choice of the acceptor and the blocking layer beneath the cathode (e.g., BCP), as excitons which are created within the acceptor can be blocked at the common interface. Although no common interface between acceptor and blocking layer at the anode exists, the choice of the acceptor material is also of importance for the strength of the blocking effect at the anode interface. This can be explained by looking at the IPCE characteristics. For PHJ devices, substituting C₆₀ with C₇₀ the absorption characteristic changes completely and thus the IPCE (inset Fig. 4(b)). As C₇₀ also strongly absorbs in the same region as DBP does, there is redistribution in absorption appearing in the IPCE curves, meaning that less excitons are generated within the DBP, while parasitic absorption occurs within the acceptor. As a consequence, the gain in J_{SC} by introducing blocking layers beneath the donor is only half as big as in the case of C₆₀ as acceptor (Fig. 4(b)). Hence, as the small increase in V_{OC} and FF is retained for this material combination, we got an increase in PCE of 19%. This result shows that the success of introducing blocking layers at the anode interface depends strongly on the choice of materials. The more absorption occurs in the donor, the more gain in PCE can be achieved.

While the gain in PCE for PHJ devices is decreased using C₇₀ instead of C₆₀, it is just vice versa for PM-HJ solar cells (Fig. 4(c)). However, this is not explained by blocking reasons and therefore a higher gain in J_{SC} . On the contrary, compared to the reference without blocker (filled circles) even a small decrease in J_{SC} is observed. Though, this deficit is easily compensated by an increase of fill factor from 56% to 60%. Due to the gain in V_{OC} an increase in PCE of 12% is reached leading to an overall efficiency of $5.8\% \pm 0.2\%$. Thus, for small molecule organic photovoltaic cells we could show that—depending on the choice of the buffer layer and the D/A combination—also for PM-HJ solar cells a remarkable efficiency enhancement is possible, introducing suitable blocking layers at the anode interface.

This work was supported by the German Research Foundation (DFG) within the priority program SPP 1355 (“Elementary Processes of Organic Photovoltaics”), by the Bavarian State Ministry of Science, Research and the Arts within the collaborative research network “Solar Technologies go Hybrid” and the Bavaria California Technology Center (BaCaTeC). S.G. and U.H. acknowledge the Bavarian Research Foundation for Ph.D. scholarships.

- ¹P. Peumans, V. Bulovic, and S. R. Forrest, *Appl. Phys. Lett.* **76**, 2650 (2000).
- ²H. Gommans, B. Verreet, B. P. Rand, R. Muller, J. Poortmans, P. Heremans, and J. Genoe, *Adv. Funct. Mater.* **18**, 3686 (2008).
- ³S. Naka, H. Okada, H. Onnagawa, and T. Tsutsui, *Appl. Phys. Lett.* **76**, 197 (2000).
- ⁴A. Steindamm, M. Brendel, A. K. Topczak, and J. Pflaum, *Appl. Phys. Lett.* **101**, 143302 (2012).
- ⁵Y. Zhou, T. Taima, T. Kuwabara, and K. Takahashi, *Adv. Mater.* **25**, 6069 (2013).
- ⁶M. Hirade and C. Adachi, *Appl. Phys. Lett.* **99**, 153302 (2011).
- ⁷D. Fujishima, H. Kanno, T. Kinoshita, E. Maruyama, M. Tanaka, M. Shirakawa, and K. Shibata, *Sol. Energy Mater. Sol. Cells* **93**, 1029 (2009).
- ⁸X. Xiao, K. J. Bergemann, J. D. Zimmerman, K. Lee, and S. R. Forrest, "Small-Molecule Planar-Mixed Heterojunction Photovoltaic Cells with Fullerene-Based Electron Filtering Buffers," *Adv. Energy Mater.* (published online).
- ⁹D. Yokoyama, Z. Q. Wang, Y.-J. Pu, K. Kobayashi, J. Kido, and Z. Hong, *Sol. Energy Mater. Sol. Cells* **98**, 472 (2012).
- ¹⁰D.-H. Lee, Y.-P. Liu, K.-H. Lee, H. Chae, and S. M. Cho, *Org. Electron.* **11**, 427 (2010).
- ¹¹A. Wilke, J. Endres, U. Hörmann, J. Niederhausen, R. Schlesinger, J. Frisch, P. Amsalem, J. Wagner, M. Gruber, A. Opitz, A. Vollmer, W. Brütting, A. Kahn, and N. Koch, *Appl. Phys. Lett.* **101**, 233301 (2012).
- ¹²A. C. Dürr, F. Schreiber, M. Münch, N. Karl, B. Krause, V. Kruppa, and H. Dosch, *Appl. Phys. Lett.* **81**, 2276 (2002).
- ¹³D. Kurrle and J. Pflaum, *Appl. Phys. Lett.* **92**, 133306 (2008).
- ¹⁴J. Wagner, M. Gruber, A. Hinderhofer, A. Wilke, B. Bröker, J. Frisch, P. Amsalem, A. Vollmer, A. Opitz, N. Koch, F. Schreiber, and W. Brütting, *Adv. Funct. Mater.* **20**, 4295 (2010).
- ¹⁵S. Kowarik, A. Gerlach, S. Sellner, F. Schreiber, L. Cavalcanti, and O. Kononov, *Phys. Rev. Lett.* **96**, 125504 (2006).
- ¹⁶M. B. Casu, S.-A. Savu, B.-E. Schuster, I. Biswas, C. Raisch, H. Marchetto, T. Schmidt, and T. Chasse, *Chem. Commun.* **48**, 6957 (2012).
- ¹⁷K. Cnops, B. P. Rand, D. Cheyns, and P. Heremans, *Appl. Phys. Lett.* **101**, 143301 (2012).
- ¹⁸M. Gruber, M. Rawolle, J. Wagner, D. Magerl, U. Hörmann, J. Perlich, S. V. Roth, A. Opitz, F. Schreiber, P. Müller-Buschbaum, and W. Brütting, *Adv. Energy Mater.* **3**, 1075 (2013).
- ¹⁹N. Koch, A. Elschner, J. Schwartz, and A. Kahn, *Appl. Phys. Lett.* **82**, 2281 (2003).
- ²⁰J. Wagner, M. Gruber, A. Wilke, Y. Tanaka, K. Topczak, A. Steindamm, U. Hörmann, A. Opitz, Y. Nakayama, H. Ishii, J. Pflaum, N. Koch, and W. Brütting, *J. Appl. Phys.* **111**, 054509 (2012).
- ²¹J. J. M. Halls, C. A. Walsh, N. Greenham, E. A. Marseglia, R. Friend, S. C. Moratti, and A. Holmes, *Nature* **376**, 498 (1995).
- ²²G. Yu, J. Gao, J. C. Hummelen, F. Wudl, and A. J. Heeger, *Science* **270**, 1789 (1995).
- ²³J. Xue, B. Rand, S. Uchida, and S. Forrest, *Adv. Mater.* **17**, 66 (2005).
- ²⁴Z. Wang, D. Yokoyama, X.-F. Wang, Z. Hong, Y. Yang, and J. Kido, *Energy Environ. Sci.* **6**, 249 (2013).